

## SEISMIC PROTECTION OF MASONRY AND INFILLED FRAME BUILDINGS USING UPGRADED SLIDING ISOLATION SYSTEM WITH SF DEVICES

Jelena Ristic<sup>(1)</sup>, Valon Veseli<sup>(2)</sup>, Labeat Misini<sup>(3)</sup>, Danilo Ristic<sup>(4)</sup>

- <sup>(1)</sup> Assoc. Prof. Dr. Faculty of Engineering, Department of Civil Engineering, International Balkan University (IBU), Skopje, Republic of North Macedonia, e-mail: [risticjelenaiibu@gmail.com](mailto:risticjelenaiibu@gmail.com)
- <sup>(2)</sup> PhD student, Faculty of Civil Engineering, Ss. Cyril and Methodius University, Skopje, Republic of North Macedonia, e-mail: [valon.veseli@uni-pr.edu](mailto:valon.veseli@uni-pr.edu)
- <sup>(3)</sup> PhD student, Institute of Earthquake Engineering and Engineering Seismology (IZIIS), Ss. Cyril and Methodius University, Skopje, Republic of North Macedonia, e-mail: [labeat.misini@gmail.com](mailto:labeat.misini@gmail.com)
- <sup>(4)</sup> Full Prof. Dr., Institute of Earthquake Engineering and Engineering Seismology (IZIIS), Ss. Cyril and Methodius University, Skopje, Republic of North Macedonia, e-mail: [danilo.ristic@gmail.com](mailto:danilo.ristic@gmail.com)

### Abstract

Presented in this paper is an innovative, uniform seismic protection system of masonry and infilled frame buildings created on the basis of a specifically upgraded sliding isolation system with new SF devices. The new building sliding-space flange protection system (BSSF system) represents a specific research segment of the integral research project, led by the fourth author, conducted in the Institute of Earthquake Engineering and Engineering Seismology (IZIIS), Ss. Cyril and Methodius University (Skopje), during three and a half years, in the frames of the innovative NATO Science for Peace and Security Project “Seismic Upgrading of Bridges in South-East Europe by Innovative Technologies (SFP: 983828)”, involving five European countries. The upgraded, seismically isolated sliding system with integrated space flange (SF) energy dissipation (ED) devices has been developed as a mechanical passive concept to provide harmonized response of building structures to strong earthquakes. It is formulated as an adaptive system, which follows the adopted concept of global optimization of seismic energy balance, through utilization of newly designed dissipation devices as a supplementary damping level to the building isolation. The new BSSF protection system is based on obligatory incorporation of the following three integrated complementary systems: (1) Sliding seismic isolation (SSI) system, (2) SF seismic energy dissipation (ED) system and (3) Earthquake displacement limiting (EDL) system. The proposed seismically resistant BSSF building system represents a qualitatively new strategy for construction of modern masonry and framed masonry buildings by applying traditional and new construction materials and providing simultaneously: (1) Full seismic safety of protected buildings, (2) Reduction of construction time, and (3) Profitable construction in seismic areas achieved by the special system characteristics.

*Keywords: building, masonry, framed masonry, seismic isolation, energy dissipation*

### 1. Introduction

The need for more successful protection of specifically targeted buildings is becoming clearly evident considering the recorded heavy damages or total failure of these structures during the latest earthquakes that have occurred worldwide (Japan, Turkey, South Europe, China, the USA, Italy, Taiwan, Chile, New Zealand, etc.). The important initial studies in the field are fully documented in the published systematic review of seismic base isolation research [1]. For the last several decades, the most renowned research centers worldwide have been making continuous efforts toward reducing catastrophic earthquake consequences through improvement and advancement of the regulations for design and construction of structures in seismically active regions, [2-6]. To increase the energy dissipation performances of the system, specific U-shaped steel dampers have been studied and recommended for application in base-isolated structures, [7-9]. Also, various earthquake damaging phenomena have been experimentally studied to define possible solution options, [10-12]. Most of the latest research projects have been initiated based on published reports on recent post-earthquake investigations of earthquake

consequences related to existing various types of structures, [13-15]. Recently, extensive research involving costly shaking table tests on constructed large-scale models have been conducted by the first author and her collaborators, mainly targeted to seismic upgrading of isolated structures with specific energy dissipation devices, [16-18]. The needed basic concept of design and construction of reduced scale models for the considered complex shaking table tests carried out under simulated earthquakes, was successfully adopted considering the data available from a completed similar research, [19]. The applied response modification method for seismic upgrading of new and existing structures actually offers a very wide potential for practical application, particularly if refined nonlinear models and specific expert analysis procedures are consistently used, [20-21]. Presented in this paper is the developed innovative, multi-directional and uniform system applicable for advanced seismic protection of masonry and infilled frame masonry buildings. The new building-sliding space flange (BSSF) system was created based on adopted advanced upgrading of the initial sliding isolation system with the created new, efficient and experimentally proved SF energy dissipation devices.

## 2. The New BSSF Isolation System

A long-term experimental and analytical study was performed in the Institute of Earthquake Engineering and Engineering Seismology (IZIIS), Ss. Cyril and Methodius University (Skopje), as part of the NATO Science for Peace and Security Project “Seismic Upgrading of Bridges in South-East Europe by Innovative Technologies” (SFP: 983828), led by the fourth author. The developed BSSF system represents a specific product of the extended part of the integrated research.

The new uniform building-sliding space flange system (BSSF-system) has been developed based on the created compact passive SF energy dissipation device providing uniform multi-directional response and improved upgrading of buildings under very strong earthquakes. It has been formulated by implementation of the adopted concept of global optimization of the seismic energy balance. The designed SF energy dissipation devices used as supplementary damping represent a qualitative system improvement in respect to the building isolation only. The BSSF system is based on incorporation of three complementary systems: (1) Basic seismic isolation system (SI system) providing low stiffness in horizontal direction; (2) The new SF energy dissipation system to provide sufficient damping through dissipation of seismic energy, and, (3) Building displacement limiting (DL) devices to reduce or eliminate excessive displacements under strong impact effects.

## 3 Prototypes of SF Devices

The new seismic energy dissipation system installed in the tested BSSF building prototype model was composed of the developed advanced steel space flange (SF) energy dissipation (ED) devices. Up till now, SF-ED dissipation devices of the proposed type have been studied only by the first author and her collaborators for bridges, [16] and [22].

Table 1. Nonlinear model properties of SF-ED-M11 and SF-ED-M12 devices computed by using the formulated nonlinear FEM model and simulated cyclic displacements with increasing amplitudes

No.	SF-ED Device M11: SF-ED-8C-L1R-T1			SF-ED Device M12: SF-ED-4C-L1R-T1		
	Notation	FEM model	(%)	Notation	FEM model	( $\Delta$ %)
1	DY (mm)	5.0	100.0	DY (mm)	6.0	120.0
2	FY (kN)	21.0	100.0	FY (kN)	9.0	42.8
3	K0 (kN/mm)	4.0	100.0	K0 (kN/mm)	1.5	37.5
4	K1 (kN/mm)	0.18	100.0	K1 (kN/mm)	0.02	11.1
5	K1/K0	0.045	100.0	K1/K0	0.013	28.8

In this paper, the two basic types of SF-ED devices are presented (Table 1). The first SF device is composed of eight ED components, model M11, representing the SF-ED-8C-L1R-T1 device, Fig. 1.

The second SF device consists of four ED components, model M12, representing the SF-ED-4C-L1R-T1 device, Fig. 2. Adopting the experimentally verified refined 3D nonlinear analytical model, the hysteretic responses of the assembled prototype devices exposed to cyclic loads have been computed successfully, Fig. 3. With the computed original results, it was confirmed that the adopted representative bilinear analytical model could be implemented to realistically model the full hysteretic behavior of the device. The defined parameters of the representative bilinear models are comparatively presented in Table 1.

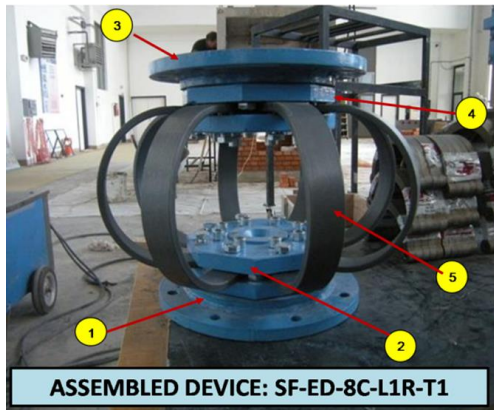


Fig. 1. Assembled SF-ED device type-1 (SF-ED-8C-L1R-T1): (1) lower base plate; (2) lower support plate; (3) upper base plate; (4) upper support plates; (5) SF-ED component

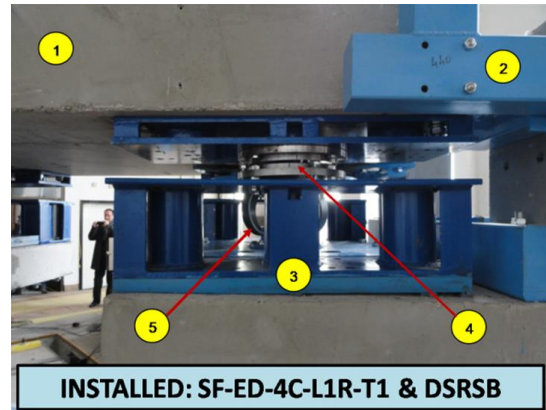


Fig. 2. Installed SF-ED device type-2 (SF-ED-4C-L1R-T1): (1) superstructure; (2) steel support of DL-device; (3) steel support of DSSSB device; (4) DSSSB device; (5) SF-ED component

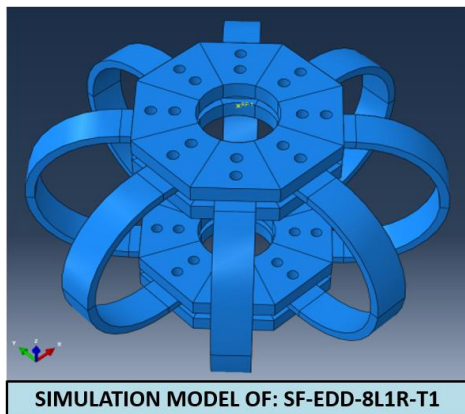
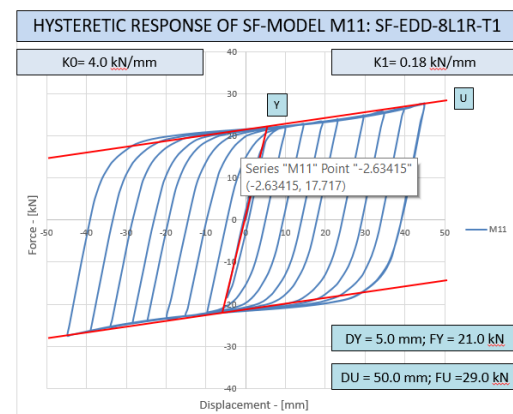


Figure 3 Modeling of the basic type-1 of the SF-ED prototype device composed of eight ED components representing the M11 prototype model.



## 4 Prototypes of Isolation and Displacement Limiting Devices

### 4.1 Prototypes of DSSSB isolation devices

The present isolation system used for the experimental BSSF model was assembled by use of the developed models of double spherical sliding seismic bearing (DSSSB) devices with two large-radii of spherical surfaces (Fig. 4).

The DSSSB devices were originally designed, constructed and used in a previous investigation carried out by Ristic, J., et al., 2017, [16]. The targets that were set prior to the design and construction of the device were fulfilled: (1) very small horizontal reaction and friction forces (reaching maximum 4.3% of the vertical load), and (2) stable hysteretic behavior along the entire range of large displacements. It was confirmed that the hysteretic behavior of the implemented DSSSB devices could be successfully simulated with the experimentally defined representative bilinear analytical model.

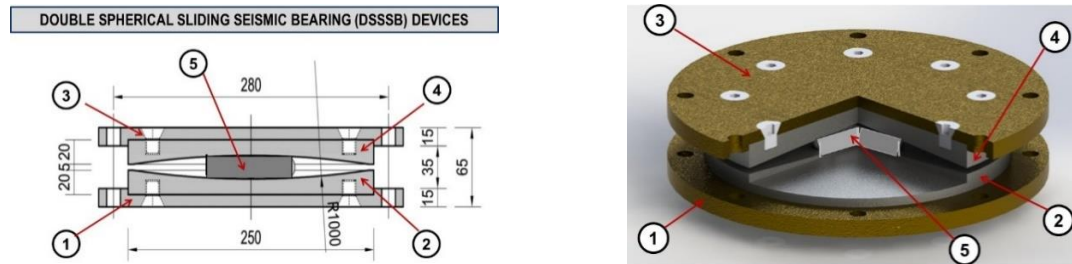


Figure 4. Basic elements of the constructed and used prototypes of DSSSB devices: (1) lower end metal plate; (2) lower spherical plate; (3) upper end metal plate; (4) upper spherical plate; (5) metallic slider;

Actually, the model was controlled by four parameters,  $DY=1.0$  mm,  $FY=0.32$  kN,  $DU=50.0$  mm,  $FU=0.92$  kN, defined experimentally under simulated vertical load and cyclic displacements with increasing amplitudes.

#### 4.2 Displacement limiting devices

The DL system implemented in the tested BSSF model consisted of built-in four limiting devices marked by (6) in Fig. 7. The implemented DL devices were installed with a predefined gap. In practice, the new, specially designed and experimentally tested rubber buffers [18] can be an advanced solution.

## 5 Seismic Tests on Large-Scale BSSF Model

### 5.1 Construction of BSSF prototype model

The original design and construction of the test model of the innovative BSSF building prototype, Fig. 5 and Fig. 6, represented a complex and specific process, specifically focused on assuring conditions for realistic experimental simulation of pre-defined important testing objectives. The three basic datasets, including (a) the main characteristics of the BSSF building model; (b) the available size of the seismic shaking table and (c) the implemented instrumentation system of the BSSF building model, were considered accordingly. Regarding the shaking table dimensions, its loading capacity and related characteristics, a geometric scale factor,  $l_r$ , of 1:4 was adopted. In order to preserve the model similarity, all the other characteristics related to the dynamic tests needed to be properly scaled. Considering the important factors addressed, the combined true replica-artificial mass simulation model was adopted as the most adequate. The scale factors for different physical quantities were defined as a function of the geometrical scale factor, according to the similitude law, [16] and [19]. The building prototype model, Fig. 5, Fig. 6 and Fig. 7, was constructed with dimensions of  $a=314.0$  cm and  $b=174.0$  cm at plan, while the considered total model height was  $h=231.0$  cm. The frame system of the model consisted of RC columns (8) with section dimensions 12.0 cm x 12.0 cm, horizontal RC beams, in both directions, with section dimensions 12.0 cm x 12.0 cm and two integrating monolithic RC slabs with thickness of 8.0 cm, spaced between the RC beams. The masonry walls (9) having characteristic door and window openings (10), were constructed using plain brick with a width of 9.0 cm. The model-base isolated monolithic RC slab (7) was constructed with thickness of 15.0 cm. The upper part of the building model (the superstructure part) rested on four DSSSB devices (4) placed on constructed four special steel spacers (3). At both ends, between the DSSSB isolators, the two new SF devices for energy dissipation were installed (5), as indicated in Fig. 7.



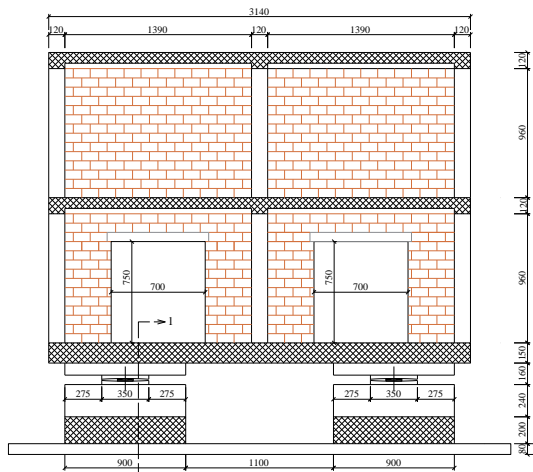


Figure 5. Side view of the designed and seismically tested BSSF large-scale prototype model.

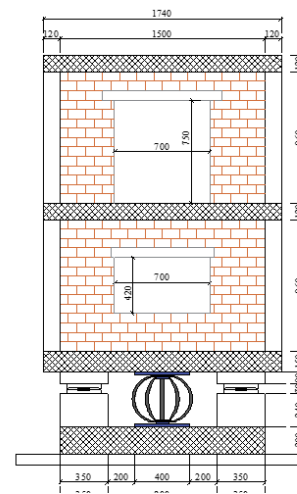


Figure 6. Front view of the designed and seismically tested BSSF large-scale prototype model.

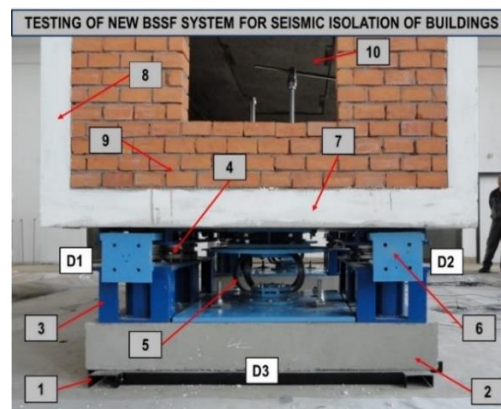


Figure 7. Isolation system of the BSSF model: Position of the installed four DSSSB devices (4), the new two assembled SF-ED devices (5) and the implemented four DL devices (6).

Similarly, at each model end, there were provided two DL devices in a cylindrical form that were tested before as special rubber buffers, (6). The integral BSSF system was supported by two RC slabs (2), proportioned 90 x 150 x 20 cm, connected to the integrating base-metal frame (1), fixed to the seismic shaking table. Eight metal elements with bulk density of 400 kg each were installed on the three RC model slabs to appropriately increase the total mass of the model. Their distribution per story was 2+2+4. The DL devices were installed at 50mm gaps to prevent the destructive effects of possible excessive displacements. All steel parts were manufactured to a reduced scale by use of S355 steel material, while concrete C25/30 was used for construction of all RC parts of the constructed model. The existing laboratory seismic shaking-table was square-shaped (5.0 by 5.0 m). Seismic input could be applied in one horizontal and in vertical direction. To adapt the large-scale BSSF model for seismic testing, its longitudinal axis was positioned to coincide with the direction of motion of the shaking table (Fig. 8). In that way, generation of seismic forces was enabled in longitudinal direction of the BSSF model. The BSSF test model was integrally assembled on the shaking table and equipped with the defined instrumentation system. For seismic testing of the BSSF prototype model, the model superstructure (isolated building) rested on four DSSSB isolators spaced at the two model ends (using pairs of devices at each end), Fig. 7 and Fig. 8. The two SF energy dissipation devices were installed at the respective middle positions, between the seismic isolators, Fig. 7.

## 5.2 Instrumentation of BSSF prototype model

To ensure acquisition of all the required data during the conducted dynamic tests, a well-designed instrumentation system was installed. The BSSF large-scale prototype model assembled on the seismic shaking table was experimentally tested under compressed real strong earthquakes, according to the model scaling and similarity conditions. The selected strong earthquakes were simulated in the considered representative longitudinal direction of the constructed model. Actually, the designed instrumentation system of the model consisted of three different types of sensors, Fig. 8 and Fig. 7:

(a) *Transducers of the type of LVDT, representing displacement sensors:* Three displacement sensors were installed to measure relative displacements in longitudinal direction. The first two transducers of the type of LVDT, marked as D1 and D2, were used for recording time histories of relative displacements between the base-support of the isolation system and the bottom RC model slab located just above the seismic isolation devices. In addition, the third transducer of the type of LVDT, marked as D3, was used to measure possible relative displacements between the shaking table and the lowest fixed steel segment supporting the entire model structure;

(b) *Transducers of the type of LP, representing linear potentiometers:* Six sensors of the type of LP were used to measure the total displacements of the isolated building model in longitudinal direction. The first two transducers marked as L1 and L2 were located on the left and the right side of the bottom RC model slab, the next two transducers, L3 and L4, were installed on the left and the right side of the middle RC slab, and the last two transducers, L5 and L6, were spaced at respective locations on the top RC model slab. To assure conditions for such measurement, the second ends of the linear potentiometers were connected to the provided appropriate connection points. The required connection points were located in the constructed additional steel frame directly fixed to the existing, nonexcited, laboratory floor, spaced with a respective gap around the moving shaking table.

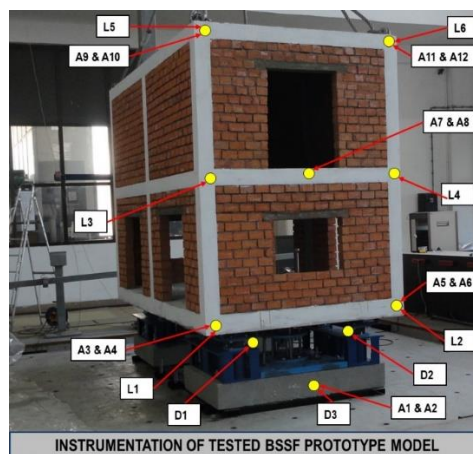


Figure 8. Acquisition points with sensors and recording channels for the BSSF large-scale prototype model tested on the seismic shaking table under simulated strong earthquakes.

(c) *Transducers of the type of ACC, representing acceleration sensors:* A total of twelve sensors of the type of ACC were installed, providing thus a pair of sensors at each of the selected six characteristic locations. The first and the second ACC sensor at each considered location were properly directed to measure acceleration time-histories in longitudinal (L) and transversal (T) direction, respectively. In the first (the lowest) ACC location, there were provided two measuring channels (A1 & A2), recording accelerations in longitudinal (L) and transversal (T) direction, respectively. Following the same instrumentation concept, at each of the next five ACC locations, two measuring channels were similarly provided. The first and the second channel (A<sub>i</sub> & A<sub>j</sub>) at each location were similarly used for recording accelerations in longitudinal (L) and transversal (T) direction, respectively.

### 5.3 Seismic shaking table tests of BSSF prototype model

(a) **BSSF Model assembling:** The innovative BSSF prototype model shown in Fig. 8 was appropriately assembled, incorporating four DSSSB isolation devices, two new SF energy dissipation devices and four displacement limiting (DL) devices, Fig. 7. The created SF energy dissipation devices were composed by installation of pre-defined four prototypes of energy dissipation components. Table. 1.

(b) **Tests with sine-sweep:** The dynamic tests carried out by simulated sine-sweep dynamic inputs, 0.02g and 0.04g, covering a range of frequencies from 1 to 35Hz and the use of the provided data sources, enabled definition of: (1) the initial fundamental period amounting to  $T_0=0.461s$ , corresponding to the case of the building model with installed DSSSB devices only. The new SF devices were not connected and not activated; and (2) Damping between 3.0 and 3.4%.

(c) **Comparative testing:** To assess the contribution of the SF devices to energy dissipation, the model was first tested with installed DSSSB isolators only, under simulated Petrovac earthquake scaled to  $PGA = 0.47 g$ . The comparative relative displacements recorded under equal test conditions for the system composed with and without SF devices are presented in Fig. 10. It was shown that the building model with installed SF devices represented a highly favorable upgrading option. For the system with seismic isolation only, an unacceptable relative displacement amounting to  $D_e = 42.6 mm$  was obtained. This excessive response actually represented the critical state, because the displacement limit of the used seismic isolators was 40.0 mm. However, regarding the BSSF system with the new SF devices, the relative displacement was reduced to a fully controlled value of  $D_c = 24.21 mm$ , representing an important reduction of -65.3%.

#### (d) Summary of testing conditions and selected results, including:

d1) **Seismic input:** Seismic testing of the new BSSF building model was carried out using four selected real earthquake records. Actually, to obtain representative experimental data, representative earthquake intensities were considered in all testing cases. The seismic input intensities were generated considering controlled high (possible) values of peak ground accelerations amounting to  $PGA=0.44g$  for the El Centro (1940) record,  $PGA=0.47g$  for the Petrovac (Montenegro, 1979) record,  $PGA=0.49g$  for the Landers record and  $PGA=0.27g$  for the Northridge record, respectively. Following the similitude law, the original earthquake records were time compressed for a time factor of  $1/2$ , as a square root of  $I_r$ .

Table 2. Maximum positive and negative relative displacements recorded by the installed LVDT sensors, during the conducted four original seismic tests of the new BSSF prototype model

No.	O-T1: C-El-Centro, PGA=0.44G			O-T2: C-Petrovac, PGA=0.47G		
	Channel	MaxD (-) (mm)	MaxD (+) (mm)	Channel	MaxD (-) (mm)	MaxD (+) (mm)
1	LVDT-01	-26.85	27.34	LVDT-01	-21.77	21.17
2	LVDT-02	-29.31	28.50	LVDT-02	-24.21	21.46
3	LVDT-03	-0.87	0.64	LVDT-03	-0.72	0.30
No.	O-T1: C-Landers, PGA=0.49G			O-T2: C-Northridge, PGA=0.27G		
	Channel	MaxD (-) (mm)	MaxD (+) (mm)	Channel	MaxD (-) (mm)	MaxD (+) (mm)
1	LVDT-01	-25.15	27.17	LVDT-01	-30.71	19.13
2	LVDT-02	-28.45	28.61	LVDT-02	-34.28	19.84
3	LVDT-03	-0.89	0.64	LVDT-03	-0.89	0.51

d2) **Data acquisition:** Extensive experimental data files were recorded from each acquisition channel. The integral data recording system included the full set of 21 channels instrumented with sensors according to the model instrumentation plan and additional extra sensors were used for full control of the shaking table.

Having such an extensive instrumentation system and refined data sampling rate from each seismic test, about 5 million numerical values were recorded. The testing process consisting of nine seismic tests, was completed very successfully and all sensors provided correct and complete experimental records continuously. The representative results showing the actual system response were selected, presented and discussed.

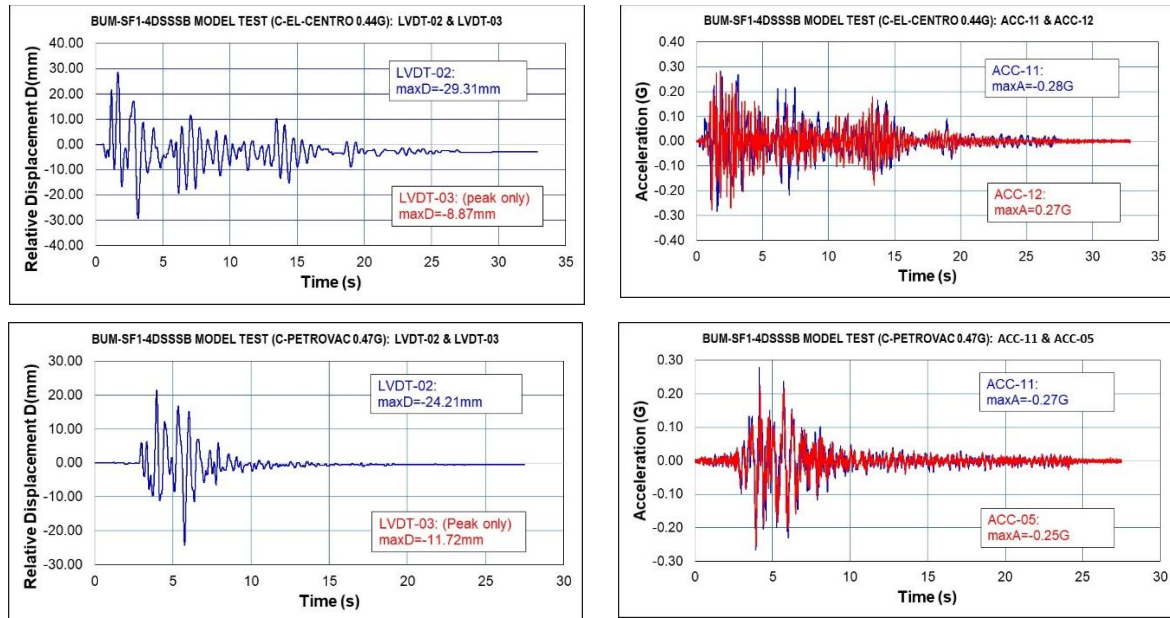


Figure 9. Relative displacements of the BSSF model-base (left) and recorded acceleration responses by ACC-11 & ACC-12 (right) during the tests carried out under simulated El-Centro and Petrovac earthquake.

Table 3. Maximum positive and negative displacements recorded by the installed LP sensors during the conducted four original seismic tests of the new BSSF prototype model

No.	O-T1: C-El-Centro, PGA=0.44G			O-T2: C-Petrovac, PGA=0.47G		
	Channel	MaxD (-) (mm)	MaxD (+) (mm)	Channel	MaxD (-) (mm)	MaxD (+) (mm)
1	LP-01	-44.04	36.98	LP-01	-21.38	16.64
2	LP-02	-44.69	37.26	LP-02	-22.41	15.74
3	LP-03	-45.62	37.65	LP-03	-22.50	17.48
4	LP-04	-44.55	40.19	LP-04	-23.30	16.55
5	LP-05	-46.45	38.31	LP-05	-23.27	17.96
6	LP-06	-46.88	36.91	LP-06	-24.00	16.93

No.	O-T1: C-Landers, PGA=0.49G			O-T2: C-Norhtrige, PGA=0.27G		
	Channel	MaxD (-) (mm)	MaxD (+) (mm)	Channel	MaxD (-) (mm)	MaxD (+) (mm)
1	LP-01	-15.44	21.60	LP-01	-51.97	39.77
2	LP-02	-16.91	20.28	LP-02	-53.58	39.89
3	LP-03	-16.74	22.90	LP-03	-53.32	40.76
4	LP-04	-17.83	21.59	LP-04	-54.46	41.10
5	LP-05	-17.53	23.62	LP-05	-54.17	41.63
6	LP-06	-18.57	22.08	LP-06	-55.73	40.31



Table 4. Maximum positive and negative accelerations recorded by the installed ACC sensors during the conducted four original seismic tests of the new BSSF prototype model

No.	Channel	O-T1: C-El-Centro, PGA=0.44G				O-T2: C-Petrovac, PGA=0.47G				
		MaxA G (-)	DAF	MaxA G (+)	DAF	Channel	MaxA G (-)	DAF	MaxA G (+)	DAF
1	ACC-01	-0.37	0.84	0.44	1.00	ACC-01	-0.48	1.02	0.39	0.82
2	ACC-02	-0.08	0.18	0.09	0.20	ACC-02	-0.06	0.12	0.08	0.17
3	ACC-03	-0.29	0.65	0.33	0.75	ACC-03	-0.28	0.59	0.21	0.44
4	ACC-04	-0.19	0.43	0.27	0.61	ACC-04	-0.23	0.48	0.29	0.61
5	ACC-05	-0.28	0.63	0.26	0.59	ACC-05	-0.25	0.53	0.22	0.46
6	ACC-06	-0.19	0.43	0.28	0.63	ACC-06	-0.22	0.46	0.30	0.63
7	ACC-07	-0.22	0.50	0.25	0.56	ACC-07	-0.20	0.42	0.19	0.40
8	ACC-08	-0.23	0.52	0.23	0.52	ACC-08	-0.29	0.61	0.23	0.48
9	ACC-09	-0.30	0.68	0.35	0.79	ACC-09	-0.25	0.53	0.28	0.59
10	ACC-10	-0.28	0.63	0.28	0.63	ACC-10	-0.38	0.80	0.32	0.68
11	ACC-11	-0.28	0.63	0.28	0.63	ACC-11	-0.26	0.55	0.27	0.57
12	ACC-12	-0.27	0.61	0.27	0.61	ACC-12	-0.37	0.78	0.33	0.70

No.	Channel	O-T1: C-Landers, PGA=0.49G				O-T2: C-Norridge, PGA=0.27G				
		MaxA G (-)	DAF	MaxA G (+)	DAF	Channel	MaxA G (-)	DAF	MaxA G (+)	DAF
1	ACC-01	-0.50	1.02	0.44	0.89	ACC-01	-0.19	0.70	0.29	1.07
2	ACC-02	-0.07	0.14	0.08	0.16	ACC-02	-0.05	0.18	0.05	0.18
3	ACC-03	-0.32	0.65	0.29	0.59	ACC-03	-0.26	0.96	0.26	0.96
4	ACC-04	-0.25	0.51	0.26	0.53	ACC-04	-0.16	0.59	0.23	0.85
5	ACC-05	-0.26	0.53	0.32	0.65	ACC-05	-0.24	0.88	0.27	1.00
6	ACC-06	-0.26	0.53	0.26	0.53	ACC-06	-0.16	0.59	0.24	0.88
7	ACC-07	-0.22	0.44	0.23	0.46	ACC-07	-0.20	0.74	0.23	0.85
8	ACC-08	-0.24	0.48	0.23	0.46	ACC-08	-0.12	0.44	0.13	0.48
9	ACC-09	-0.32	0.65	0.35	0.71	ACC-09	-0.24	0.88	0.29	1.07
10	ACC-10	-0.37	0.75	0.35	0.71	ACC-10	-0.15	0.55	0.26	0.96
11	ACC-11	-0.34	0.69	0.31	0.63	ACC-11	-0.26	0.96	0.29	1.07
12	ACC-12	-0.37	0.75	0.35	0.71	ACC-12	-0.14	0.51	0.25	0.92

(d3) *Relative displacements*: The relative peak displacements, including positive and negative pulses, recorded during the seismic tests of the BSSF system under the simulated El-Centro, Petrovac, Landers and Northridge earthquake are presented in Table 2. Comparatively, Fig. 9 (left) shows the recorded time-histories of relative displacement responses in longitudinal (L) direction during the tests carried out by simulation of the El-Centro and Petrovac earthquake, respectively. Regarding the presented experimental results, the following important observations were made: (1) The recorded relative displacements in L direction (direction of earthquake excitation) were dominant; (2) It was confirmed that the test model was successfully fixed to the shaking table since the relative displacements in L direction recorded by LVDT-03 were very small in all test cases. (3) The absolute maximum recorded relative displacement amounting to  $D_{max} = 34.28$  mm was below the critical (allowable) relative displacement of the seismic isolators amounting to  $D_a = 40.0$  mm, and (4) Generally, the seismic response of the assembled BSSB system that was tested repeatedly appeared to be very similar twice. The results from the conducted original series of tests-1 are presented (O-Ti in Table 2). Consequently, the series of repeated seismic tests-2 (not presented) were realized using the same four earthquakes. Only small, negligible differences of maximum displacements were observed.

(d4) *Accelerations*: The representative time-histories of accelerations recorded by sensors ACC-11 and ACC-12, respectively in L and T-direction, during the seismic tests on the BSSF model conducted under the simulated El-Centro and Petrovac earthquakes are comparatively shown in Fig. 9 (right).

However, Table 4 shows the representative peak accelerations recorded by all sensors, namely, ACC-01 to ACC-12. At each measuring point, accelerations were recorded in L and in T-direction during the seismic tests on the BSSF model conducted under the simulated all four representative earthquakes. Considering the presented results, it was confirmed that: (1) The recorded accelerations at the superstructure, respectively in L and T-direction, were quite small (without amplification); and (2) Due to the present regular fluctuation, the recorded accelerations at the superstructure in L and T-direction were with similar peak values and in the expected range; (3) The new BSSF system showed sustainability since the response parameters recorded during the original (O) tests-1 and the repeated tests-2 were quite similar, and (4) Generally, the DAF (dynamic amplification factor) values presented in the same Table 4 were quite small (smaller than 1.0), demonstrating favorable and consistent response. It was confirmed that the obtained relations between the maximum response and the maximum input acceleration ( $DAF = A_r/PGA$ ) were within the expected ranges in all cases.

(d5) *Absolute displacements:* The absolute displacement responses (in L -direction) recorded by the six LP sensors, Table 4, installed on the BSSF model, proved existence of small inter-story drifts and successful control of the shaking table in all realized testing cases.

(d6) *System advances:* Generally, the new BSSF system exhibited safe and very favorable behavior under strong earthquake excitations. Considering the processing of more than 50.000.000 recorded original numerical values obtained from the realized fifteen shaking table tests, the main qualitative advances of the innovative GHS system upgraded with SF energy dissipation devices, are summarized in Fig. 10. Stable, reliable and safe seismic response was observed in all test cases due to the provided significant reduction of maximum relative displacements amounting to 36.5%, 65.3%, 39.8% and 16.7%, respectively, in the case of the simulated El Centro, Petrovac, Landers and Northridge earthquakes. All recorded peak values were lower than the defined allowable design displacement of  $D_a=40.0\text{mm}$  for the seismic isolators. The importance of upgrading the isolated masonry and infilled frame buildings with the new SF devices was experimentally validated and confirmed with the conducted initial quantification test of the model with the installed seismic isolation only. Under the simulated strong Petrovac earthquake, the tested system without SF devices showed an unsafe response to the recorded excessive relative displacement amounting to  $\text{max}D=42.6\text{ mm}$ , Fig. 10.

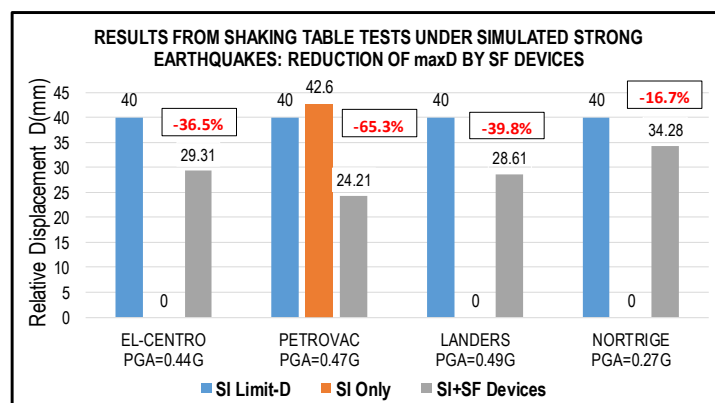


Figure 10. Advances of the BSSF system: Reduction of maximum relative displacements defined from the conducted seismic tests under simulated strong earthquakes.

## 6 Conclusions

Based on the results obtained from the conducted extensive experimental study, the following conclusions are drawn: (1) The new building-sliding space-flange (BSSF) system represents a favorable, efficient and experimentally proved option for seismic protection of masonry and framed masonry buildings.

The system shows a quite significant modification of the seismic response of the integral structure, resulting directly in efficient protection of buildings subjected to repeated and very strong earthquakes; (2) The originally designed, constructed and implemented double spherical sliding bearing (DSSSB) devices were confirmed as favorable types of isolation bearings for the new BSSF isolation system. However, the other developed and proved advanced types of isolation bearings may also be regarded as a potentially good application option; (3) The created new uniform space-flange energy dissipation devices (SF-ED) exhibited a very good and stable energy dissipation capacity. Their perfect capability to exhibit smooth and stable hysteretic response under arbitrary earthquake excitation was clearly confirmed. In addition, the new SF energy dissipation devices preserve their dissipation capability even in the cases of strong repeated cyclic earthquake loading; (4) The displacement limiting (DL) devices of the building should be considered as an obligatory constituent element of the created BSSF system serving as the last defense line against excessive displacements of the integral building. Their appropriate design is an important step toward providing their activation only in the critical cases of very strong and abrupt earthquakes; (5) The three-dimensional, hysteretic, uniform and multi-directional response of the new SF energy dissipation devices can be very successfully predicted by advanced application of the nonlinear micro-modeling concept with the adopted bilinear kinematic hardening steel material model; (6) The present study resulted in development of an experimentally proved basic concept required for successful elaboration of the advanced design procedure. The developed design concept can assure practical application of the new BSSF system providing a qualitatively upgraded seismic protection capability of masonry and framed masonry buildings located in seismic regions.

## Acknowledgements

The present study represents a supplemental part of the long-term innovative NATO Science for Peace and Security Project: Seismic Upgrading of Bridges in South-East Europe by Innovative Technologies (SFP: 983828). The extended NATO support to the realization of the extensive innovative research is highly appreciated.

## REFERENCES

- [1] Kelly, J. M. (1986): Aseismic Base Isolation: A Review and Bibliography, *Soil Dynamics and Earthquake Engineering* 5, 202-216. [DOI]
- [2] Robinson, W. H. (1982): Lead-Rubber Hysteretic Bearings Suitable for Protecting Structures During Earthquakes, *Earthquake Engineering and Structural Dynamics* 10, 593-604. [DOI]
- [3] Iemura, H., Taghikhany, T., Jain, S. K. (2007): Optimum Design of Resilient Sliding Isolation System for Seismic Protection of Equipment, *Bulletin of Earthquake Engineering* 5, 85-103. [DOI]
- [4] Zayas, V. A., Low, S. S., Mahin, S. A. (1990): A Simple Pendulum Technique for Achieving Seismic Isolation, *Earthquake Spectra* 6, 317-334. [DOI]
- [5] Mokha, A., Constantinou, M. C., Reinhorn, A. M. (1990): Teflon Bearings in Seismic Base Isolation I: Testing, *Journal of Structural Engineering* 116, 438-454. [DOI]
- [6] Skinner, R. I., Kelly, J. M., Heine, A. J. (1975): Hysteretic Dampers for Earthquake Resistant Structures, *Earthquake Engineering and Structural Dynamics* 3, 287-296. [DOI]
- [7] Ene, D., Yamada, S., Jiao, Y., Kishiki, S., Konishi, Y. (2017): Reliability of U-shaped Steel Dampers Used in Base-Isolated Structures Subjected to Biaxial Excitation, *Earthquake Engineering & Structural Dynamics* 46, 621-639. [DOI]
- [8] Oh, S., Song, S., Lee, S., Kim, H. (2013): Experimental Study of Seismic Performance of Base-Isolated Frames with U-shaped Hysteretic Energy-Dissipating Devices, *Engineering Structures* 56, 2014-2027. [DOI]
- [9] Jiao, Y., Kishiki, S., Yamada, S., Ene, D., Konishi, Y., Hoashi, Y., Terashima, M. (2014): Low Cyclic Fatigue and Hysteretic Behavior of U-shaped Steel Dampers for Seismically Isolated Buildings under Dynamic Cyclic Loadings, *Earthquake Engineering Structural Dynamics* 44(10): 1523-1538. [DOI]

- [10] Jankowski, R., Seleemah, A., El-Khoribi, S., Elwardany, H. (2015): Experimental Study on Pounding between Structures During Damaging Earthquakes, *Key Engineering Materials* Vol. 627, 249-252. [DOI]
- [11] Serino, G., Occhiuzzi, A. (2003): A Semi-Active Oleodynamic Damper for Earthquake Control: Part 1: Design, Manufacturing and Experimental Analysis of the Device. *Bulletin of Earthquake Engineering* 1: 269–301. [DOI]
- [12] Tian, L., Fu, Z., Pan, H., Ma, R., Liu, Y. (2019): Experimental and Numerical Study on the Collapse Failure of Long-Span Transmission Tower-Line Systems Subjected to Extremely Severe Earthquakes, *Earthquakes and Structures* 16 No. 5. [DOI]
- [13] UNCRD (1995): Comprehensive Study of the Great Hanshin Earthquake, UNCRD Research Report Series No. 12, United Nations Centre for Regional Development (UNCRD), Nagoya, Japan.
- [14] Ghasemi, H., Cooper, J. D., Imbsen, R., Piskin, H., Inal, F., Tiras, A. (2000): The November 1999 Duzce Earthquake: Post- earthquake Investigation of the Structures on the TEM, Publication No. FHWA-RD-00-146, Federal Highway Administration Report.
- [15] Erdik, M. (2001): Report on 1999 Kocaeli and Duzce (Turkey) Earthquakes, *Structural Control for Civil and Infrastructure Engineering*, pp. 149-186 (2001). [DOI]
- [16] Ristic, J., Misini, M., Ristic, D., Guri, Z., Pllana, N. (2017): Seismic Upgrading of Isolated Bridges with SF-ED Devices: Shaking Table Tests of Large-Scale Model, *Gradjevinar*, 2147-2017. [DOI]
- [17] Ristic, J., Brujic, Z., Ristic, D., Folic, R., Boskovic, M. (2021): Upgrading of Isolated Bridges with Space-Bar Energy-Dissipation Devices: Shaking Table Test, *Advances in Structural Engineering*, June 23, 2021; pp. 2948–2965.
- [18] Ristic, J. (2016): Modern Technology for Seismic Protection of Bridge Structures Applying Advanced System for Modification of Earthquake Response, PhD Thesis, Institute of Earthquake Engineering and Engineering Seismology (IZIIS), “SS Cyril and Methodius” University, Skopje, Macedonia.
- [19] Candeias, P., Costa, A. C., Coelho, E. (2004): Shaking Table Tests of 1:3 Reduced Scale Models of Four-Story Unreinforced Masonry Buildings, 13th World Conference on Earthquake Engineering, Vancouver, Paper: 2199.
- [20] Ristic, D. (1988): Nonlinear Behavior and Stress-Strain Based Modeling of Reinforced Concrete Structures Under Earthquake Induced Bending and Varying Axial Loads, Doctoral Dissertation, School of Civil Engineering, Kyoto University, Japan.
- [21] Ristic, D., Ristic J. (2012): Advanced Integrated 2G3 Response Modification Method for Seismic Upgrading of Advanced and Existing Bridges, 15th World Conf. on Earthquake Engineering, (WCEE), Lisbon.
- [22] Misini, M., Ristic, J., Ristic, D., Guri, Z., Pllana, N. (2019). Seismic upgrading of isolated bridges with SF-ED devices: Analytical study validated by shaking table testing, *GRAĐEVINAR*, 71 (4), 255-272, doi: <https://doi.org/10.14256/JCE.2274.2017>